Kinetic energy backscatter for NWP models and its calibration

Glenn Shutts

Met Office, Fitzroy Road
EX1 3PB, United Kingdom
glenn.shutts@metoffice.gov.uk

ABSTRACT

A form of kinetic energy backscatter (CASBS) has been tested in the ECMWF ensemble prediction system and shown to be an effective means of increasing forecast member spread. Better matching of model error growth to ensemble spread leads to improved probability skill scores and there is preliminary evidence that CASBS can provide this. Some physical justification for the use of kinetic energy backscatter in NWP models will be discussed here along with a strategy for quantifying its effect. As an example of this, the use of explicit cloud simulation in big domains to quantify the statistical effect of deep tropical convection will be discussed and the backscatter forcing function computed by coarse-graining model fields and determining effective Reynold's stresses.

1 Introduction

Fundamental global conservation properties of the atmosphere-ocean system such as angular momentum, energy and entropy are of great interest yet often difficult to determine from observations and in the case of entropy - hard to define and compute. The production and dissipation of kinetic energy is a small part of the global budget of energy yet is important because it relates directly to the growth and decay of weather systems. Definitions of available potential energy help to quantify how spatial variation in the radiation field can force temperature variations from which buoyancy forces can produce kinetic energy. In fact these concepts arise more naturally in the entropy budget framework rather than the energy budget. The production of large-scale available potential energy is proportional to the product of the diabatic heating rate and temperature which in all likelihood is a fairly robust quantity - independent of the kinetic energy dissipation rate. Large-scale production of kinetic energy is dominated by its conversion from available potential energy at the synoptic scale and the balance constraint (e.g. quasi-geostrophy) ensures that the energy cannot readily cascade to small scales but tends to go into meandering jetstreams and cyclones which are dissipated through the Ekman pumping effect.

In general the rate of kinetic energy dissipation in the boundary layer is probably fairly well-represented in NWP models and its global-mean is typically around 2 Wm^{-2}. Locally however the dissipation rate may have substantial errors e.g. mountainous regions where uncertainties in roughness length (and indeed the suitability of stress laws based on local equilbrium) may be large. Similarly the amount of kinetic energy dissipated in convective clouds, jetstreams and frontal zones are not known with any certainty. As suggested byLilly (1983) even a small fraction of the turbulent kinetic energy in the outflows of convective storms could, if quasi-two-dimensional, propagate upscale and influence synoptic scale flows. It is already known that the mesoscale convective storms found over continents in summer are of sufficient scale to impact directly on the baroclinically active scales.

The mathematical theory of frontogenesis based on the semi-geostrophic equation set gives a realistic picture of the process by which large-scale flow deformation acting on spatially-varying horizontal temperature

gradients can generate a singular response in the form of discontinuity surfaces emerging from the surface (Cullen & Purser (1984)). Very intense frontal gradients of wind and temperature may also form at jet-streams associated with tropopause folding. Observations suggest that discontinuity formation is prevented by shearing instability that breaks out in thin layers within frontal zones in the lower and upper troposphere (Chapman & Browning (2001)). NWP models are unable to resolve the fine scales associated with front formation and numerical smoothing effects take over as the discontinuity-limiting process.

Balanced equations sets such as the barotropic vorticity equation and Quasi-Geostrophic (QG) equations do not permit vortex stretching (only planetary vorticity can be stretched in the QG set) and so are unable to describe the mechanism that leads to fronts. As such they are unable to dissipate energy in the way that real flows do, however numerical simulations with them *will* be accompanied by energy loss through implicit or explicit numerical diffusion (required to prevent enstrophy build up). The resulting energy sink leads to an unrealistic spectral energy tail-off at short wavelengths. Frederiksen & Davies (1997) showed how the inclusion of a backscatter eddy viscosity term in barotropic vorticity equation simulations led to much improved energy levels in the spectral tail.

Energy dissipation in NWP models occurs for numerical and physical reasons and it will be argued in the next section that this kinetic energy should be re-injected into the model near the truncation scale to account for energy transfer out of the sub-grid scale and back to the resolved scale. The Cellular Automaton Stochastic Backscatter Scheme (CASBS) implemented in the ECMWF Integrated Forecast System (IFS) aims to do this by summing numerical and physical sources of sub-grid scale kinetic energy and forcing a fraction of this into the resolved scales (Shutts & Palmer (2004)). It achieves this by defining a streamfunction forcing field using a home-grown Cellular Automaton (CA) to define its spatial and temporal characteristics and modulates this with the square-root of a dissipation rate field dependent on local flow properties. The dissipation rate field is the sum of contributions to the sub-grid scale kinetic energy from numerical dissipation (i.e. horizontal diffusion and semi-Lagrangian interpolation error), mountain drag and detrainment from parametrized deep convection).

A new scheme is currently being developed at the Met Office called Stochastic Kinetic Energy Backscatter (SKEB). At present this scheme only addresses numerical error which comes mainly from using semi-Lagrangian advection. A direct evaluation of the kinetic energy lost in the interpolation step equates to a global-mean rate of loss of energy of about 0.75 Wm^{-2} i.e. a significant fraction of the global-mean of the boundary layer dissipation rate. A streamfunction forcing pattern is again used to perturb the model flow but now the pattern is derived from a random number generator and enables direct control of horizontal and vertical spatial correlation scales. The pattern evolves in time as a first-order Markov process where the auto-correlation time scale can be controlled. The amplitude of the pattern is now modulated with the local kinetic energy of the model flow and so jetstream regions receive the largest vorticity perturbations.

The purpose of this article then is to briefly review the physical motivation for stochastic backscatter in NWP models and then show some results from a Cloud-Resolving Model (CRM) which has been used to compute the effective backscatter from deep tropical convection cloud systems.

2 Sources of sub-grid scale KE and backscatter

2.1 Numerical dissipation

The idealized baroclinic wave life cycle experiments of Simmons & Hoskins (1978) provide some measure of the likely levels of dissipation in an NWP context. Their Figure 4 shows a time series plot of globally-averaged energy conversions and kinetic energy dissipation due to the effects of internal diffusion over the course of a

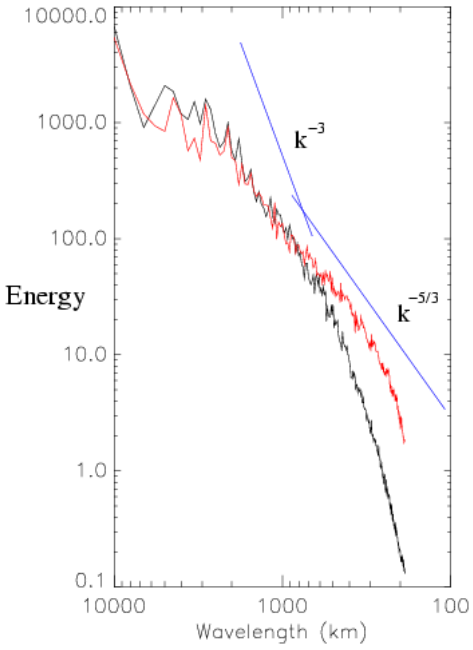

Figure 1: Kinetic energy spectrum at 500 hPa plotted versus wavelength; the black line is the control run; red line is the run with SKEB and the blue lines indicate -3 and -5/3 slopes. Day 10 of the forecast was used

baroclinic wave development and its subsequent decay. They use a spectral hyperviscosity term to smooth the fields and in the mature phase of the baroclinic wave this results in a peak global-mean dissipation rate of about 0.8 Wm^{-2} . No boundary layer parametrization was included and so energy dissipation was by the hyperviscosity term alone. Similar magnitudes of numerical dissipation rate (due to interpolation error in the semi-Lagrangian advection scheme have been found in the Met Office Unified Model (UM)). If this dissipation rate is representative of real atmospheric frontal zones (where one could expect the effect of mixing to be largest) then assuming that frontal zones occupy about one hundredth of the horizontal domain, a mean frontal KE dissipation rate of the order of 80 Wm^{-2} is implied. In an explicit calculation of the likely dissipation rates in frontal zones Blumen (1990) estimated values in the range 50 - 250 Wm^{-2}. However, observational estimates suggest much smaller values (e.g. Chapman and Browning, 2001) more typical of the boundary layer. It is possible that NWP models dissipate an order of magnitude more energy than real frontal zones in an effort to resist the scale collapse near the truncation scale. Fine structure in the wind field resulting from frontogenesis is 'lost between the gridpoints' and effectively becomes sub-gridscale balanced flow. There is no requirement that all of this energy be dissipated through the breakdown into three-dimensional turbulence and it is quite reasonable to suppose that a significant fraction of this sub-gridscale energy could be returned to the resolved scales.

The SKEB and CASBS schemes both allow for this form of energy drain and force it back into the resolved flow, though with a spatial structure determined from the random number-based pattern generator or CA respectively. Figure 1 shows the impact of the SKEB scheme when nearly all of the numerically-dissipated kinetic energy is returned to the UM resolved flow. Nastrom & Gage (1985) show from aircraft data that at wavelengths shorter than about 800 km the slope of the energy spectrum is quite close to 5/3. The black curve shows that rather than getting shallower, the spectral slope becomes steeper for scales less than 1000 km. With the addition of the backscatter term this error is reduced significantly.

2.2 Mountain drag

Turbulent kinetic energy derived from near-surface wind shear is expected to cascade to viscous scales on the order of an eddy turnover time. Large Eddy Simulation (LES) of the boundary layer is found to be improved by the inclusion of backscatter terms in the momentum equation (Mason & Thomson (1992). The net dissipation is a small residual between the parametrized energy drain rate (e.g. determined by a Smagorinsky-Lilly eddy viscosity formulation) and the backscatter term. Without the backscatter forcing the simulated mean wind profile departs markedly from the textbook 'log law'. This form of backscatter is probably not an issue for NWP and it will be assumed here that the backscattered energy associated with boundary layer eddies is negligible at the 50 km scale of forecast model resolution.

Current orographic drag parametrization schemes attempt to account for sub-gridscale drag forces on much larger scales than turbulent eddies and encompass the effects of gravity wave stress, vortex wakes and cold air damming (flow blocking) against mesoscale mountain ridges. Gravity waves radiated from orography exert a drag force where they break and this may take place within the stratosphere. The deposition of momentum accompanying the wave stress leads to potential vorticity (PV) anomalies whose scale presumably matches the scale of the mountain range that forced them. Vortex wakes and flow blocking will also be accompanied by quasi-two-dimensional PV anomalies and these will tend to transfer energy upscale rather than downscale. However, as far as an NWP model is concerned, the parametrized drag force is associated with an energy sink for the resolved flow. The energy lost from the resolved flow is implicitly assumed to be converted to thermal energy (some mountain drag parametrizations include a matching thermal increment, others neglect it).

2.3 Deep convection

Kinetic energy released by buoyancy forces in convective clouds may be dissipated in turbulence; radiated away as gravity waves, or may remain after the convection has stopped as balanced flow associated with a potential vorticity anomaly. For boundary layer convection most of the energy is dissipated in turbulent eddies whereas deep convection, particularly that organized at the scale of mesoscale convective systems, generates mesoscale potential vorticity anomalies that may persist long after convection ceases. Under these conditions Shutts & Gray (1994) suggest that as much as 30% of the kinetic energy released in deep convection may be trapped in residual balanced flow.

Since NWP convective parametrizations were never designed to reproduce the individual effect of mesoscale convective systems, the use of backscatter algorithms to describe the injection of KE into the resolved scales of a forecast model seems justifiable. Indeed Gray (2001) has tested such a stochastic convective vorticity forcing scheme in the Met Office Unified Model and found small but significant impacts on forecast evolution by day 5. The scheme works by injecting circular vorticity perturbations into the model flow where there is substantial convective instability. The scale and intensity of the perturbations is functionally related to the Convective Available Potential Energy (CAPE) and the local Coriolis parameter and their location is selected randomly with these high CAPE regions. The biggest effects of convective forcing on forecast evolution occur when the vorticity perturbations are located near jetstreams.

2.4 Backscatter algorithms for NWP

The numerical and physical sources of energy backscatter identified above can be brought together using the concept of a *total sub-gridscale dissipation rate* to quantify the transfer of energy from resolved scales to sub-grid scales. In the ECMWF CASBS scheme, estimates of the numerical and mountain drag dissipation rates are added to the rate of kinetic energy detrainment implied by the convective parametrization scheme (Shutts

(2005)). The square-root of this total dissipation rate (D) is used to set the amplitude of a streamfunction forcing (F_ψ)) in the defining relation:

$$F_\psi = \frac{1}{2}\alpha\Delta s \cdot \Psi\sqrt{\Delta\tau \cdot D}/\Delta\tau \tag{1}$$

where α is a tuning constant, Δs and $\Delta\tau$ are the CA gridlength and time step respectively and Ψ is a time-evolving pattern function that determines the spatial and temporal form of the vorticity forcing. In the case of CASBS, Ψ is determined from a cellular automaton and in its most general usage the CA would be functionally related to the forecast model flow fields.

In principle, the same type of expression could be used to force the horizontal divergence although this would generate gravity wave motion and therefore would be potentially less effective.

3 Calibration of convective backscatter using a cloud-resolving model

In order to quantify the statistical properties of F_ψ the Met Office cloud-resolving model has been configured to run in equatorial beta-plane geometry covering an area 7680 km x 7680 km, centred on the equator and spanning a latitude range ± 35 degrees. A working assumption has been that gridlengths less than or equal to 2 km are necessary for deep convection simulations yet the computation burden of a uniform 2 km grid or finer on this domain is too great. It was also considered to be important to span the entire meridional extent of the tropics. Rather than use a narrow strip domain (although such a configuration has been tested with 1 km resolution) it was felt best to use an anisotropic grid with 2 km resolution in x and 10 km resolution in y. For the purposes of analysing the statistical effect of clouds at the 100 km scale it is not expected that this grid anisotropy will have a major influence.

The model is forced by a uniform tropospheric cooling rate of 1.5 K/day above a fixed sea surface temperature (SST). The chosen form for the SST pattern represents the decrease in temperature with latitude and includes an east-west component that roughly describes the observed relative warmth over the west tropical Pacific area and cooler east Pacific. A Trade Wind forcing function is introduced as a fixed sink of westerly momentum peaking at a height of 11 km and at latitudes 17 degrees north and south. Its role is to represent the effect of Rossby wave drag due to the influx of wave action from middle and high latitudes. The size of the forcing function was set so that the implied net flux of westerly momentum out of the tropics is in reasonable agreement with its observed value.

The simulation was initialized with the zonally-averaged zonal wind component, temperature and water vapour mixing ratio from an earlier simulation to minimize spin-up. Diagnostics will be shown for day 4.5 by which stage convection is active and concentrated over the model's 'warm pool' region. The potential temperature perturbation at the lowest model level ($z = 78\ m$) (Fig. 2) strongly reflects the underlying surface temperature distribution though with cooler air patches caused by convective downdraughts. Although convection occurs throughout the domain it is concentrated in a double ITCZ i.e. bands near 15 degrees north and south (though at higher latitudes in the warm pool region). In this simulation, convection is weak near the equator although in simulations without Trade wind forcing and with zonally-symmetric SSTs the double ITCZ is absent and convection is more uniformly distributed.

Fig. 3 shows two sub-tropical jetstreams that arise through thermal wind balance as the surface temperature pattern is transmitted to the atmosphere by deep convection. Convection growing in the neighbourhood of the jetstreams transport westerly momentum downwards and contribute to the total Reynolds' stresses exerted by cloud systems on the large-scale flow. The aim here is to quantify the full Reynolds' stress divergence by the following coarse-graining approach.

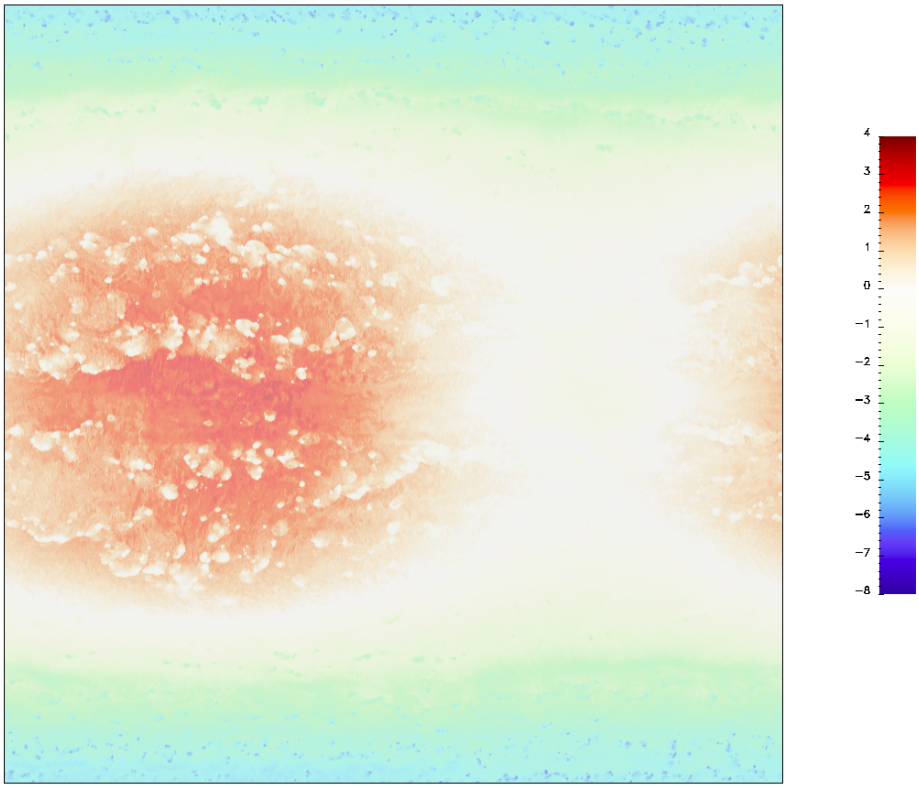

Figure 2: Perturbation temperature (K) at $z = 78$ m at day 4.5 (add 26 C to obtain the potential temperature itself)

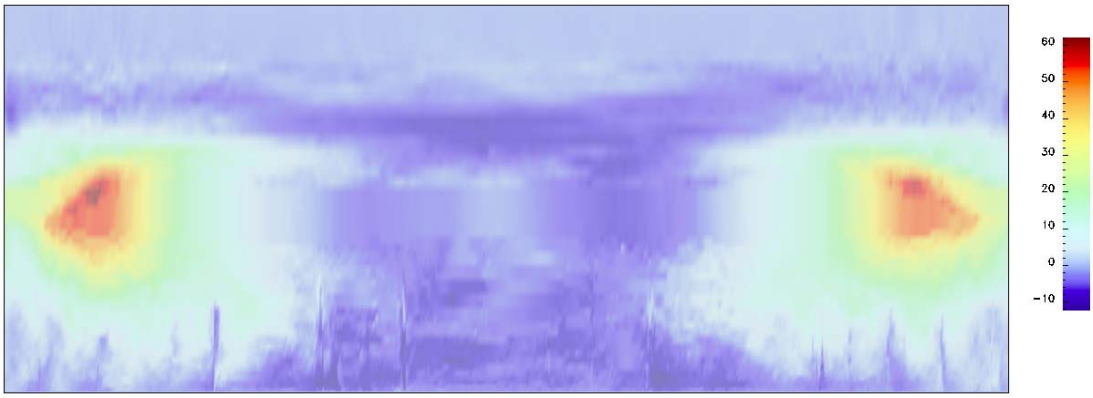

Figure 3: North-south Vertical section of u at the centre of the domain on day 4.5

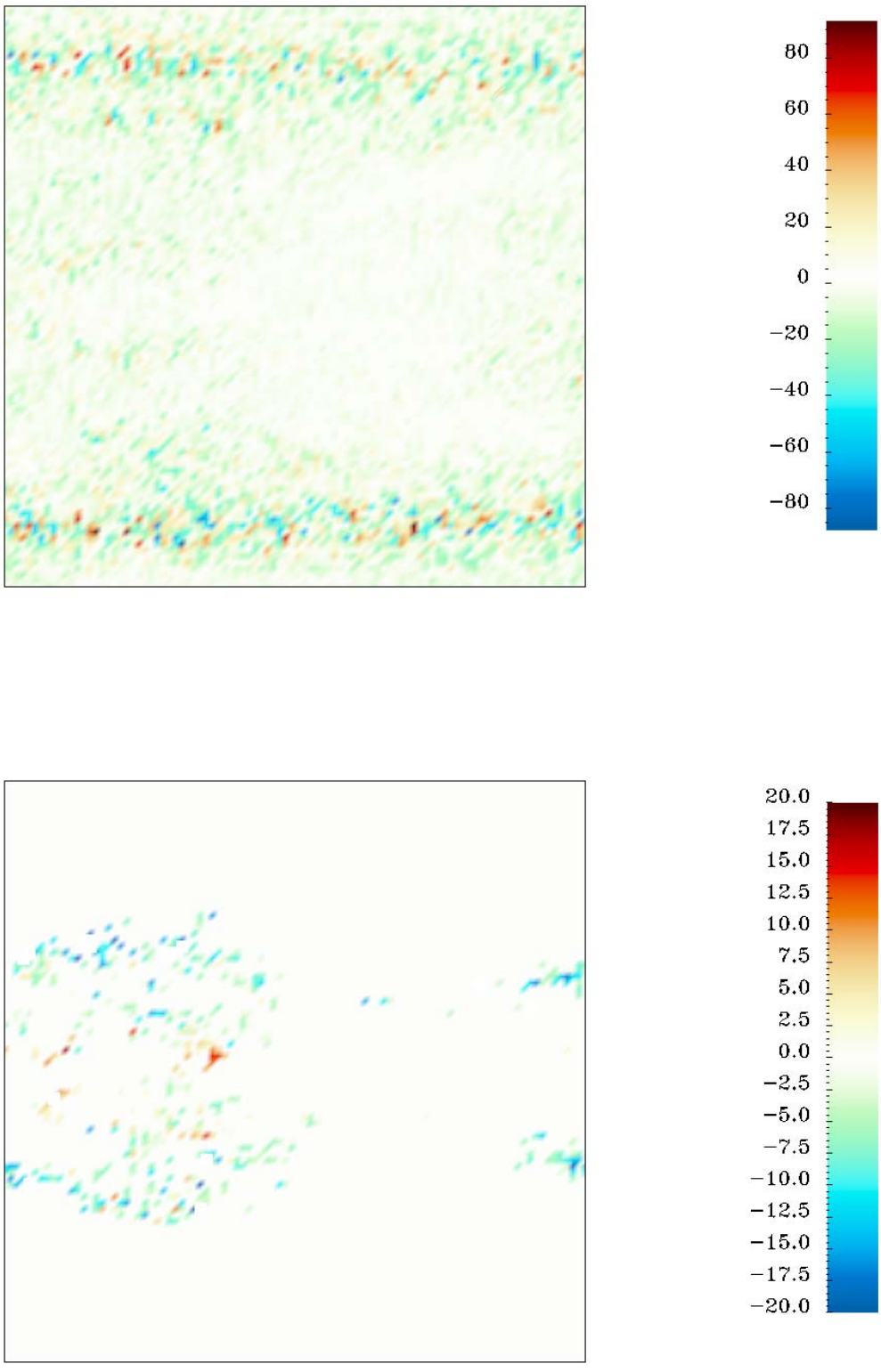

Figure 5: x-component of parametrized force (per unit mass) due to convective momentum transport at day 4.5 (ms^{-1}/day)

The momentum equation used in the cloud-resolving model can be written as:

$$\frac{\partial \mathbf{V}}{\partial t} + f\mathbf{k} \wedge \mathbf{V} + \nabla \frac{p}{\rho_0} = \mathbf{S_V}$$

where $\mathbf{V}$ is the horizontal wind vector, f is the Coriolis parameter, $\mathbf{k}$ is the unit vector pointing upwards, p is the pressure, $\rho_0(z)$ is the basic state density profile and $S_\mathbf{V}$ is the sum of the advection term $(-\mathbf{V} \cdot \nabla \mathbf{V})$ and parametrized turbulent eddy stresses. Let $\widehat{(..)}$ denote the average over a coarse gridbox then:

$$\frac{\partial \widehat{\mathbf{V}}}{\partial t} + f\mathbf{k} \wedge \widehat{\mathbf{V}} + \nabla \frac{\widehat{p}}{\rho_0} = \widehat{\mathbf{S_V}}$$

and adding $\widehat{\mathbf{V}} \cdot \nabla \widehat{\mathbf{V}}$ to each side gives

$$\frac{\partial \widehat{\mathbf{V}}}{\partial t} + \widehat{\mathbf{V}} \cdot \nabla \widehat{\mathbf{V}} + f\mathbf{k} \wedge \widehat{\mathbf{V}} + \nabla \frac{\widehat{p}}{\rho_0} = \widehat{\mathbf{S_V}} - \mathbf{S}_{\widehat{\mathbf{V}}}$$

If the coarse-grained fields like $\widehat{\mathbf{V}}$ are equated with averages over NWP model gridboxes then the Reynolds' stress divergence $\widehat{S_\mathbf{V}} - S_{\widehat{\mathbf{V}}}$ is what is required as a parametrization. Fig. 4 shows the x-component of this effective eddy forcing term seen by coarse-graining to an 80 km grid at a height of 8.8 km. Perhaps not surprisingly the largest contribution arises in the jetstream regions although the effects of deep convection over the warm pool area can also be seen.

In order to assess the extent to which convective momentum transport parametrization captures these mesoscale Reynolds' stresses the coarse-grained fields of wind, temperature and humidity were used as input to a convective parametrization scheme (Bechtold *et al.* (2001)). Fig. 5 shows the corresponding force per unit mass computed from the parametrization scheme (note the smaller range). It suggests that the jetstream contributions may not be directly due to deep convective momentum transport and that forcing is mainly in the warm pool region where convection is most intense.

The spectral power in the Reynolds' momentum forcing function is plotted in Fig. 6 and compared with the same calculation when the advection term $\widehat{\mathbf{V}} \cdot \nabla \widehat{\mathbf{V}}$ is computed using a pre-smoothed wind field. The smoothing operation is carried out in spectral space and has the response function shown in Fig. 7 which strongly filters wavelengths shorter than about 500 km. In this way the computed Reynolds' stresses contain spectral contributions in the wavelength range 160 to 500 km (which are filtered out by coarse-graining to an 80 km grid). The simulated convection contains much more energy in this range and as Fig. 8 shows, there is no clear scale separation in the energy spectrum. Peaks in momentum forcing spectral power occur at the two-gridlength wavelength (i.e. 160 km) and at wavenumber 2 for the coarse-graining procedure without pre-smoothing. With smoothing of $\mathbf{V}$ the spectral power is fairly uniform - the additional spectral power being caused by the re-definition of the filter scale. When coarse-graining CRM simulations to calibrate backscatter forcing, it seems that the latter procedure represented by the solid line in Fig.6 might be more relevant.

The spectral power in the momentum forcing function implied by the convective parametrization is given in Fig. 9. Noting that the vertical scale is 100 times smaller than in Fig. 6 it suggests that parametrized vertical stresses are only a small part of the full backscatter. It should be emphasized that the dominant component to the Reynolds' stresses comes from the jetstream region and this may only be indirectly related to the convection.

Overall, these preliminary results imply that parametrized convective momentum transport may not be accounting for the full extent of deep cloud systems on the mesoscale wind field. Even if one excludes the jetstream regions, the CRM-derived effective momentum forcing has more power than the parametrized. Clearly, at

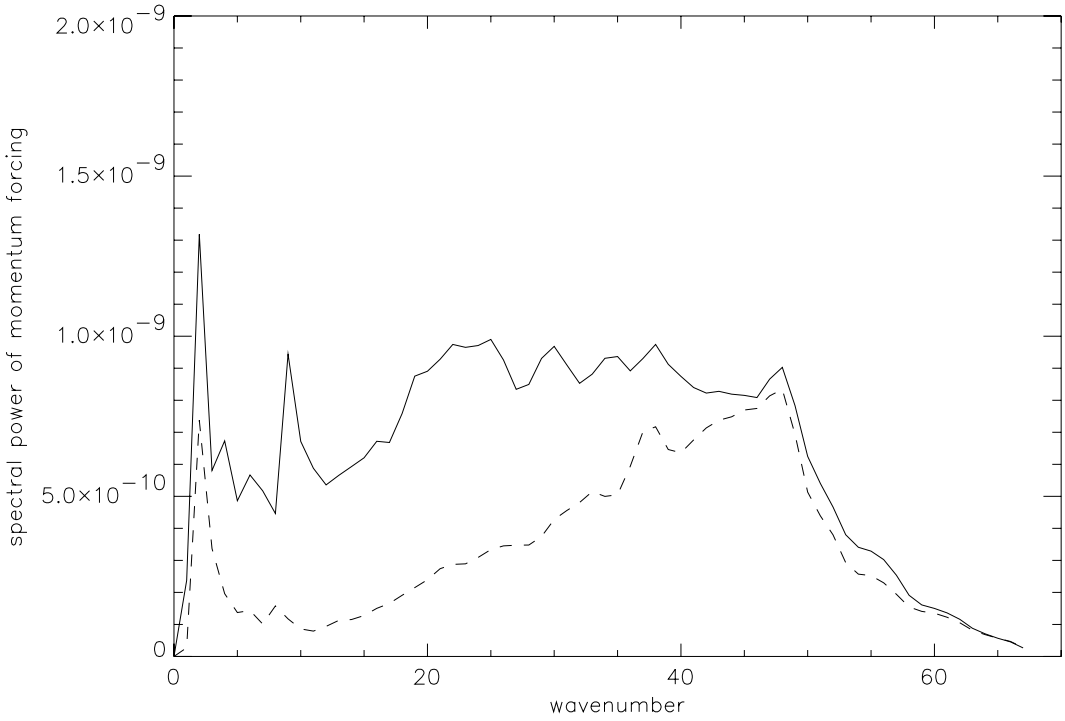

Figure 6: Spectral distribution of power in the momentum forcing function $\widehat{S_{\mathbf{V}}} - S_{\widehat{\mathbf{V}}}$ *at* $z = 8.8$ *km : (i) coarse-graining to an 80 km grid (dashed line); (ii) spectrally smoothed prior to coarse-graining onto the same grid. (solid line)*

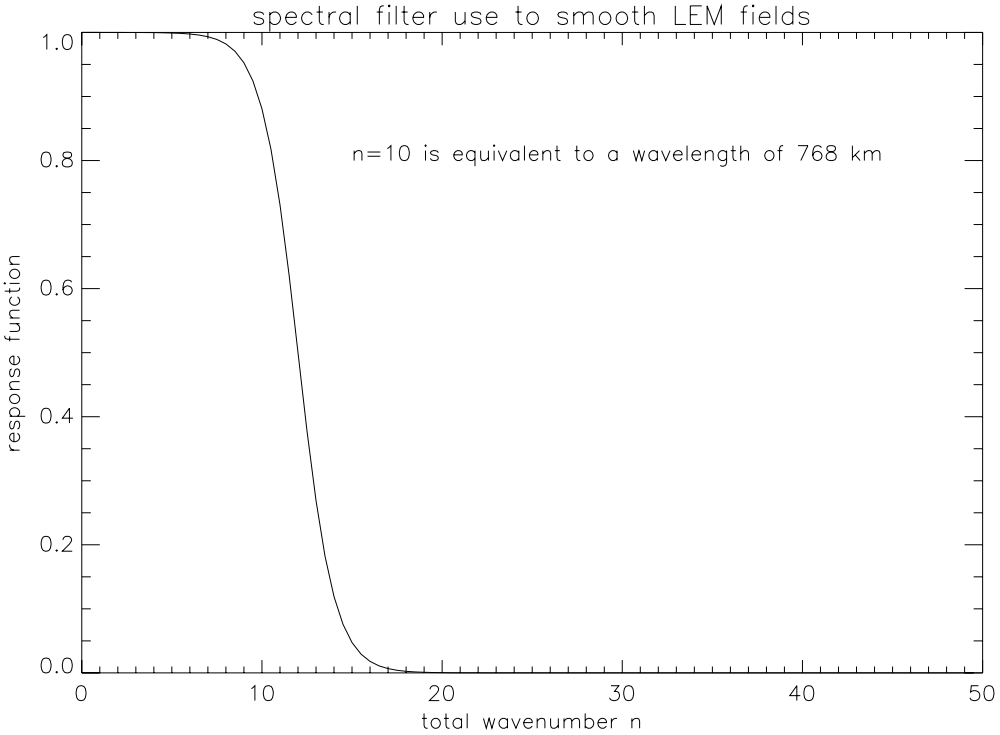

Figure 7: Spectral response function used to smooth the wind field

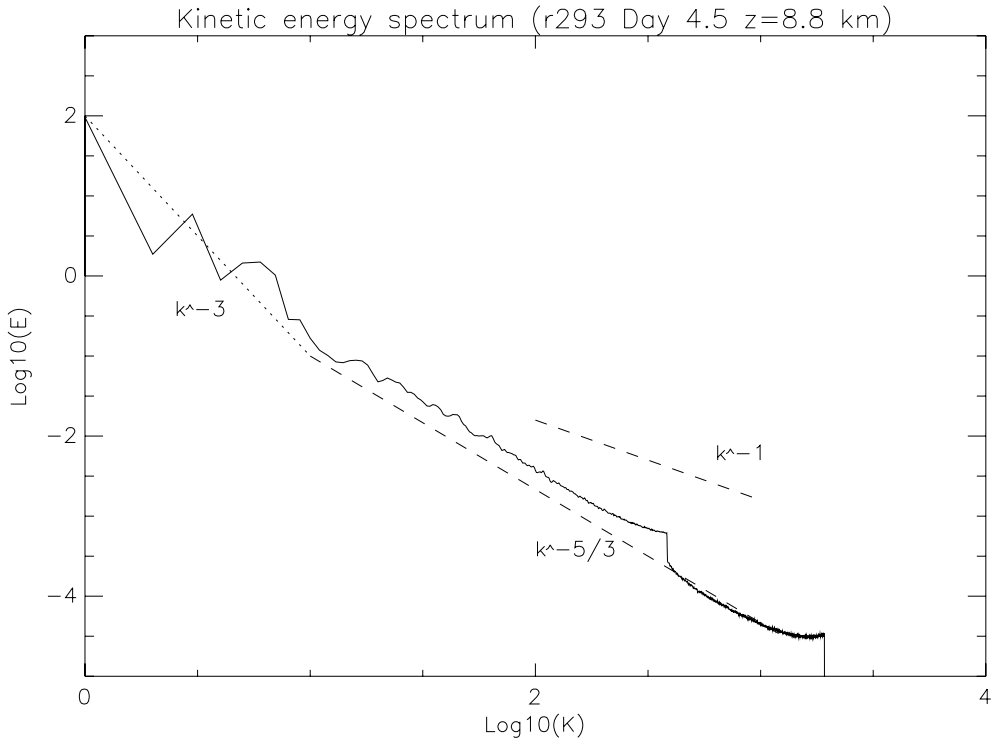

Figure 8: Energy spectrum at day 4.5

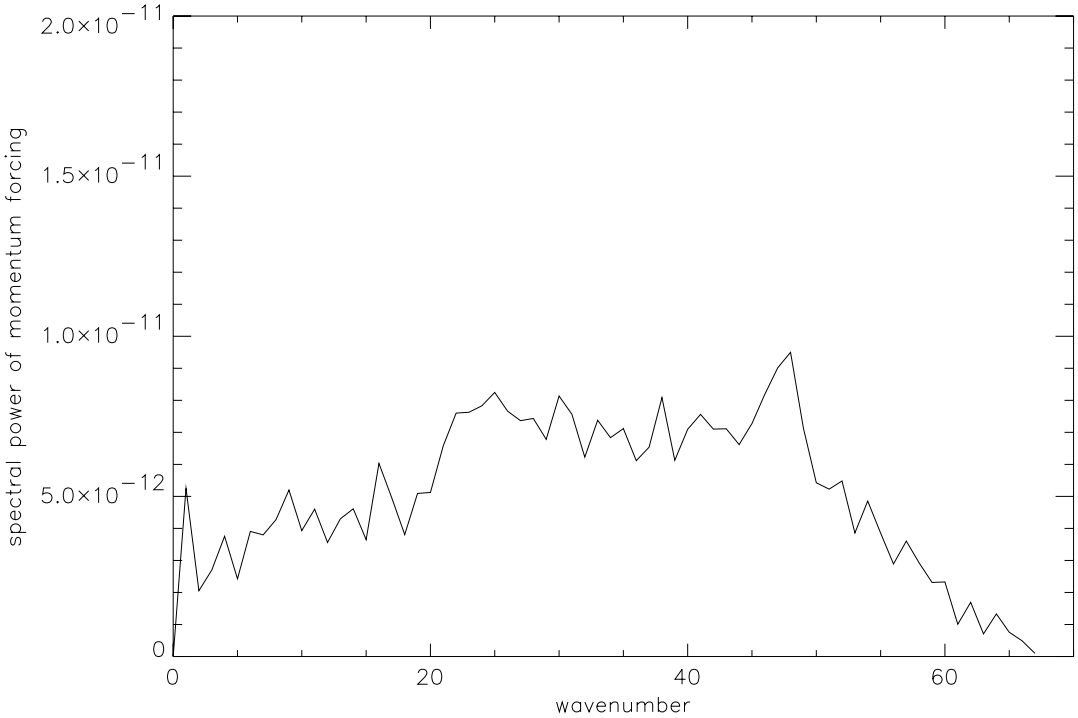

Figure 9: Spectral distribution of power in the momentum forcing function at $z = 8.8$ km implied by the convective parametrization scheme

this early stage of the data analysis it is difficult to generalize and the problem of disentangling the mesoscale convection from the balanced flow dynamics remains a difficulty. Given that the model resolution is still too coarse to accurately describe turbulent cloud dynamics, the results must be interpreted with caution.

4 Summary

It has been argued that there is an excessive drain of kinetic energy in NWP models that has its origin in numerical diffusion and mountain drag. There is mounting evidence that this should be matched by a similar magnitude (though necessarily smaller) backscatter term representing the expulsion of kinetic energy from the sub-gridscale back to the resolved scales. Also, deep convection acts as a kinetic energy source for the sub- and near gridscales of NWP models - a process that can be incorporated into the backscatter framework.

By coarse-graining high resolution CRM fields (and their associated advective tendencies) to an NWP model grid it is possible to determine the eddy forcing required to make the NWP model evolve like the coarse-grained fields of the CRM simulation. The probability distribution function of this eddy forcing, conditioned on judiciously-chosen bulk model properties (e.g. CAPE), could be used as the basis of a stochastic parametrization. Preliminary results suggest that the effects of deep convection on the large-scale momentum field may not accounted for by current convective momentum parametrization alone.

Acknowledgements

Thanks go to Tom Allen who has provided considerable technical assistance thoughout this work and Alberto Arribas for results pertaining to the SKEB scheme.

References

Bechtold, P., Bazile, E., Guichard, F., Mascart, P. & Richard, E. (2001) A mass-flux convection scheme for regional and global models. *Q.J.R. Meteorol. Soc.* **127**, 869–886.

Blumen, W. (1990) A semigeostrophic Eady-wave frontal model incorporating momentum diffusion. Part II: Kinetic energy and enstrophy dissipation. *J. Atmos. Sci.* **47**, 2903–2908.

Chapman, D. & Browning, K. A. (2001) Measurements of dissipation rate in frontal zones. *Q.J.R. Meteorol. Soc.* **127**, 1939–1959.

Cullen, M. J. P. & Purser, R. J. (1984) An extended Lagrangian theory of semi-geostrophic frontogenesis. *J. Atmos. Sci.* **41**, 1477–1497.

Frederiksen, J. S. & Davies, A. G. (1997) Eddy viscosity and stochastic backscatter parameterizations on the sphere for atmospheric circulation models. *J. Atmos. Sci.* **54**, 2475–2492.

Gray, M. E. B. (2001) The impact of mesoscale convective-system potential-vorticity anomalies on numerical-weather-prediction forecasts. *Q.J.R. Meteorol. Soc.* **127**, 73–88.

Lilly, D. K. (1983) Stratified turbulence and the mesoscale variability of the atmosphere. *J. Atmos. Sci.* **40**, 749–761.

Mason, P. J. & Thomson, D. J. (1992) Stochastic backscatter in large-eddy simulations of boundary layers. *J. Fluid Mech.* **242**, 51–78.

Nastrom, G. D. & Gage, K. S. (1985) A climatology of atmospheric wavenumber spectra of wind and temperature observed by commercial aircraft. *J. Atmos. Sci.* **42**, 950–960.

Shutts, G. J. (2005) A kinetic energy backscatter algorithm for use in ensemble prediction systems. *Q.J.R. Meteorol. Soc. to appear* .

Shutts, G. J. & Gray, M. E. B. (1994) A numerical modelling study of the geostrophic adjustment process following deep convection. *Q.J.R. Meteorol. Soc.* **120**, 1145–1178.

Shutts, G. J. & Palmer, T. N. (2004) The use of high resolution numerical simulations of tropical convection to calibrate stochastic physics schemes. *ECMWF/CLIVAR Workshop on Simulation and Prediction of Intra-Seasonal Variability with emphasis on the MJO. 3-6 November 2003* pp. 83–102.

Simmons, A. J. & Hoskins, B. J. (1978) The life cycles of some nonlinear baroclinic waves. *J. Atmos. Sci.* **35**, 414–432.